International Symposium
On Turbulence and Shear Flow
Phenomena (TSFP-8)
August 28 - 30, 2013 Poitiers, France

EFFECTS OF SPANWISE ROTATION ON THE STRUCTURE OF TURBULENT STRIPE IN PLANE POISEUILLE FLOW

Takahiro Ishida
Department of Mechanical Engineering
Tokyo University of Science
Chiba, Japan
j7512609@ed.tus.ac.jp

Takahiro Tsukahara
Department of Mechanical Engineering
Tokyo University of Science
Chiba, Japan
tsuka@rs.tus.ac.jp

Yasuo Kawaguchi
Department of Mechanical Engineering
Tokyo University of Science
Chiba, Japan
yasuo@rs.noda.tus.ac.jp

ABSTRACT

In the transitional channel flow, the large-scale intermittent structure of localized turbulence which is called turbulent stripe, can be found in the form of stripe arrangement. The structure of turbulent stripe is oblique laminar-turbulent banded pattern. We performed the direct numerical simulation at the transitional Reynolds numbers and very low-rotation numbers, and focused on the turbulent stripe in the plane Poiseuille flow subjected to spanwise system rotation. We captured the turbulent stripe in rotating channel flow and found the augmentation and diminution of the turbulent stripe affected by the spanwise rotation. The contents of the discussion are the spatial size of turbulent stripe on the basis of the instantaneous flow fields, the energy spectra, and the spanwise velocity component that characterizes the turbulent stripe. It shoud be noted that the turbulent stripe is enhanced due to the Coriolis instability and the spanwise velocity component increases, while the quasi-laminar region is wider at very low-rotation number.

INTRODUCTION

The laminar-turbulent transition state has been studied by many researchers, beginning with the pioneering experiment in pipe flow by O. Reynolds in 1883. In recent years, the intermittent structures occurring in transitional flows have attracted many researchers interest. The intermittent structures were determined in various flow fields, such as turbulent puff in pipe flow, spiral turbulence in Taylor-Couette flow. In the turbulent to laminar reverse-transitional channel flow, the large-scale intermittent structure which is called turbulent stripe (TS) was found. The structure of TS, that is oblique laminar-turbulent banded pattern and is characterized by spanwise secondary flow, is described in Tsukahara et al. (2010) by numerical simulations and Hashimoto et al. (2010) by experiment. Tsukahara et al. (2010) reported the stream- and spanwise-wavelengths of a pattern of TS as $\lambda_x^+ = \lambda_x(u_\tau/\nu) \approx 5000$ and $\lambda_z^+ = \lambda_z(u_\tau/\nu) \approx 2000$, respectively in plane Poiseuille flow (PPF) at $\mathrm{Re}_\tau(= u_\tau\delta/\nu) = 80$ (ν, the kinematic viscosity; u_τ, the friction velocity; δ, half the channel width). When the Reynolds number decreases to transitional regimes, the occurrence of TS delays transition to fully-laminar flow from turbulent flow, and maintains large energy transfer like turbulent flow in transition regime toward the laminar flow. Then, the presence of TS is an important problem for physical resolution about the transition, and for engineering application.

Brethouwer et al. (2012) indicated the occurrence of TS in the stable case of rotating plane Couette flow and magnetohydrodynamic flow, subjected to external forces such as Coriolis and Lorentz forces. This implies that fully-developed wall turbulence at transitional Reynolds numbers on in states stabilized moderately by external forces would provide a intermittent turbulence with TS. However in the rotating plane Poiseuille flow subjected to spanwise system rotation (RPPF), the presence of TS has not been discovered because the instability with roll cell (RC) dominates in terms of turbulent structures. The structure of RC is an array of large-scale longitudinal vortices aligning in the spanwise direction with regularity (Johnston et al., 1972).

As is well known, RPPF is a complicated flow field consisting of the suction side and the pressure side (see Fig. 1). The flow is stabilized and destabilized in the suction side and pressure side by the Coriolis force, respectively. Bradshaw (1969) and Lezius and Johnston. (1976) demarcated stability by Bradshae number ($\mathrm{B} = S(S+1)$, $S = 2\Omega/(\mathrm{d}\bar{u}/\mathrm{d}y)$), ($\Omega$, system angular velocity; $\bar{u}$, mean

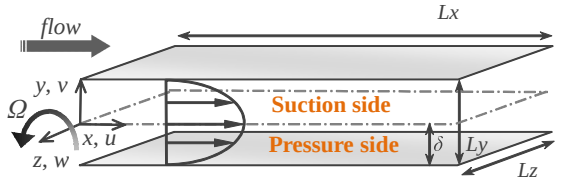

Figure 1. Configuration of plane Poiseuille flow with spanwise system rotation.

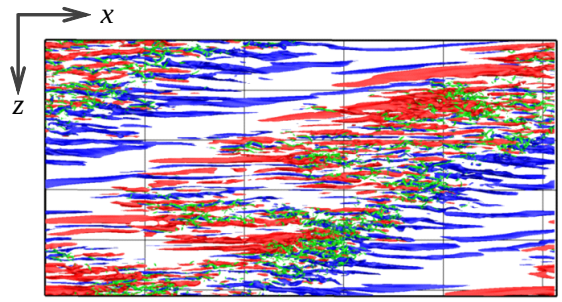

Figure 2. Visualization of instantaneous flow field at $\mathrm{Re}_\tau = 64$ and $\mathrm{Ro}_\tau = 0.01$ in the pressure side, viewed from wall-normal direction. Red isosurface, $u'^+ > 3$; blue, $u'^+ < -3$; green, $II'^+ = u'_{i,j}u'_{j,i} < -0.025$ (which equivalent to the vortical position). The mean flow moves from left to right.

streamwise velocity) and zero absolute velocity (ZAV). The flow should be stabilized or destabilized depending on B, and ZAV ($S = 2\Omega$) is the intermediate region between stabilized- and destabilized-regions. It is known that the Coriolis force has two major effects: a linear effect and a scrambling effect (Morinishi et al., 2001). In this paper, we refer to them as the direct effect and the indirect effect, respectively. If we consider the channel flow with spanwise (z) system rotation, the direct effect acts as the energy exchange between $\overline{u'u'}$ and $\overline{v'v'}$ (u', streamwise (x) velocity fluctuation; v', wall-normal (y) velocity fluctuation) through Reynolds shear stress ($\overline{u'v'}$). The indirect effect affects the nonlinear interaction between the velocity components of the rotating turbulence and inhibits the energy cascade from low to high wavenumber. Hence the indirect effect delays the decay of kinetic energy.

In our previous report, we performed the direct numerical simulation (DNS), and we found the occurrence of TS only in very low rotation number ($\mathrm{Ro}_\tau = 2\Omega\delta/u_\tau$) in RPPF (Ishida et al. 2012). In this paper, we investigate the parameter range, where TS would occur in both or one of the channel halves, by means of DNS. An emphasis is placed on the augmentation or diminution of the TS affected by the spanwise system rotation. The spatial structure size of TS is estimated by instantaneous flow fields and energy spectra, and the spanwise velocity component which characterizes TS is discussed.

NUMERICAL CONDITION

The plane Poiseuille flow with spanwise system rotation that we consider here is driven by a uniform pressure gradient in the x direction. In this case, we confirmed the coexistence of the stabilized and destabilized sides in a channel. They are classified as halves of the channel (i.e. the pressure and suction sides are the bottom and top sides, respectively) for simplicity, since the maximum of the mean velocity did not significantly change in height because of low rotation numbers. Figure 1 represents the configuration of flow field in this study. The fundamental equations are the equation of continuity and following equation of the Navier-Stokes equation:

$$\frac{\partial u_i^+}{\partial t^*} + u_j^+ \frac{\partial u_i^+}{\partial x_j^*} = -\frac{\partial p^+}{\partial x_i^*} + \frac{1}{\mathrm{Re}_\tau}\frac{\partial^2 u_i^+}{\partial x_j^* \partial x_j^*} - \mathrm{Ro}_\tau \varepsilon_{i3k} u_k^+ \quad (1)$$

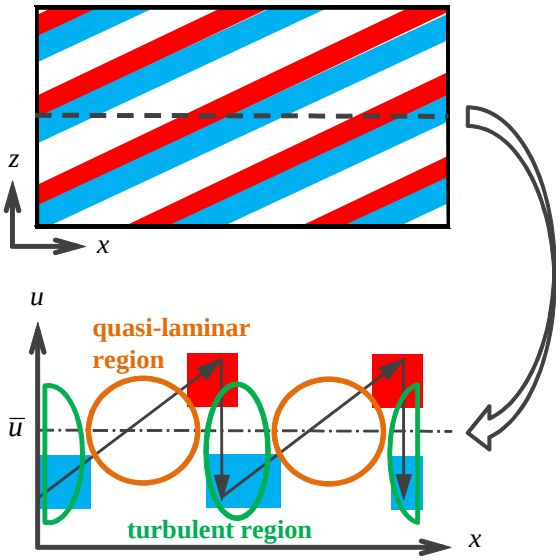

Figure 3. Diagram of the structure of turbulent stripe and the streamwise velocity. Red and blue regions represent high- and low-speed regions, respevtively.

Note that the superscripts of $+$ and $*$ indicate the quantities normalized by the wall unit and the outer scale, respectively. A term of ε_{ijk} in Eq. 1 means Eddington's epsilon. The periodic boundary conditions were imposed in the x and z directions and the non-slip condition was applied on the wall surface. The finite difference method was adopted for the spatial discretization. For the time integration, the second-order Crank-Nicolson and Adams-Bashforth schemes were used for the wall-normal viscous term and the other terms, respectively.

We performed a series of DNS for transitonal Reynolds numbers of $\mathrm{Re}_\tau = 64$ and 80, and rotation numbers $\mathrm{Ro}_\tau = 0.0$–1.5 to investigate the effect of spanwise rotation for turbulent structures. A large computational domain of $102.4\delta \times 2\delta \times 51.2\delta$ with grids of $2048 \times 192 \times 1024$ in x, y, and z directions was employed, to capture several bands of TS because the stream- and spanwise-domain of TS are roughly known in previous studies.

RESULTS

Turbulent stripe in RPPF

The occurrence of TS was found in the lower Ro_τ than those in exsisting reports for RPPF. Parameter ranges in which TS is dominant structure both in the pressure and the suction sides are $\mathrm{Ro}_\tau \leq 0.02$ for $\mathrm{Re}_\tau = 64$, and $\mathrm{Ro}_\tau \leq 0.01$ for $\mathrm{Re}_\tau = 80$. An example of snapshot of the flow field accompanied by TS is given in Fig. 2. The structure of TS consists of the quasi-laminar region and the turbulent region. These regions stably exist in alternate shifts. In the turbulent region, the vortexes densely occur between high- and low-speed streaks, and local centerline velocity is lower relatively than that in the quasi-laminar region. The quasi-laminar region (except for turbulent region) is small velocity fluctuation, and this region reveals high velocity at the channel center like laminar flow.

Figure 3 shows the diagram of TS in the (x,z)-plane and the streamwise velocity variation on the black dash line in the top figure. The structure of TS contains quasi-laminar

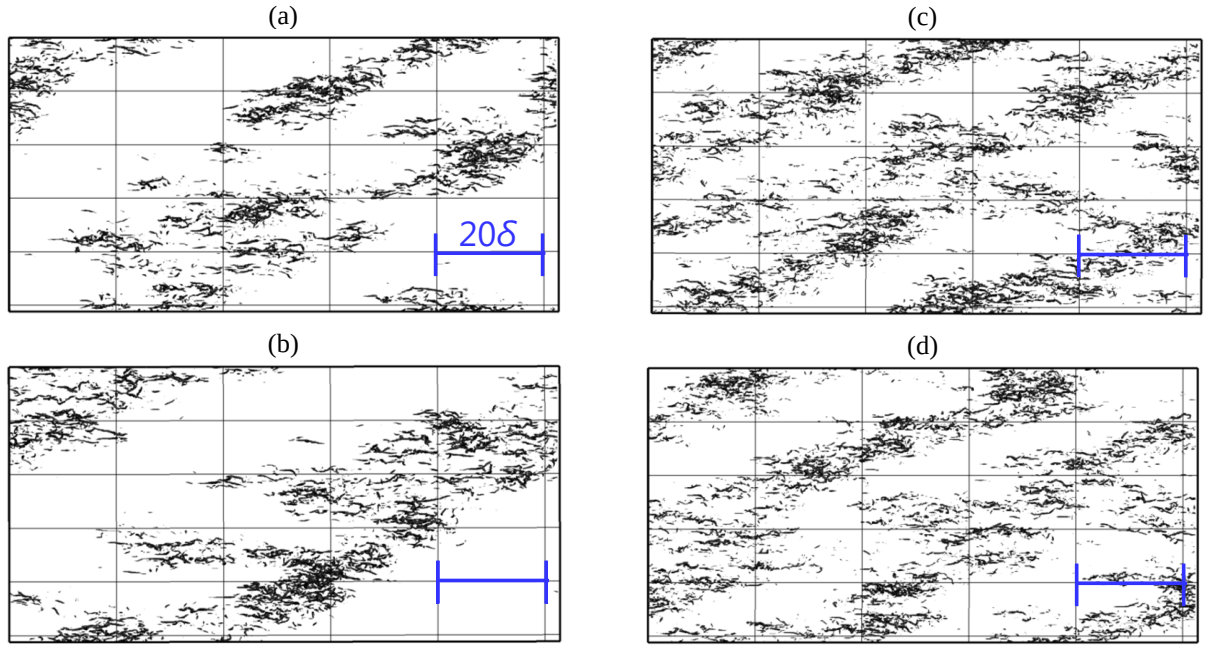

Figure 4. Visualization of instantaneous flow fields at (a) $\mathrm{Ro}_\tau = 0.0$, $\mathrm{Re}_\tau = 64$, (b) $\mathrm{Ro}_\tau = 0.02$, $\mathrm{Re}_\tau = 64$, (c) $\mathrm{Ro}_\tau = 0.0$, $\mathrm{Re}_\tau = 80$ and (d) $\mathrm{Ro}_\tau = 0.01$, $\mathrm{Re}_\tau = 80$ in the pressure side viewed from wall-normal direction (same as Fig 2). Black isosurface notes $II'^{+} = u'_{i,j}u'_{j,i} < -0.025$ (which equivalent to the vortical position). The mean flow moves from left to right.

region (high velocity), and turbulent region (low velocity), and so the quasi-laminar region impinges on the turbulent region. Then, the streamwise velocity decreases rapidly. The streamwise velocity is accelerated gently by the flow toward to the quasi-laminar region from the turbulent region. The velocity repeats the process of the rapid decrease and the gentle acceleration. In consequence, local high- and low-speed region occurs in a regular manner.

The visualization of vortexes is shown to extract the turbulent region of TS in Fig. 4. Only the pressure side is visualized, since TS occurs irrespective of the pressure- and the suction-side in the static system and very-low rotation number ranges. There is a little difference in the structure of TS in the very-low rotation number region (b, d) and the static system (a, c). Although, the densely-crowded vortex region at the very-low $\mathrm{Ro}_\tau = 0.01$ and 0,02 are clearly observed than those at $\mathrm{Ro}_\tau = 0.0$ (a, c), and the quasi-laminar region (except for vortex region) in (b, d) is wider than those in (a, c). At $\mathrm{Re}_\tau = 80$, the inclination of TS against the x direction may appear in two directions (two-way inclination), right-up and right-down directions if shown in figure as like Fig 4. In this case, the spatial region of the quasi-laminar region is narrowew than in one-way inclination (e.g. Fig. 4(b) shows only one right-up inclination). At $\mathrm{Ro}_\tau = 0.02$, TS contains only one densely-crowded vortex region such as one-way inclination, and quasi-laminar region is wider than those at $\mathrm{Ro}_\tau = 0.0$. The relation between the quasi-laminar region and the inclination of turbulent region is examined above according to visualization, however it is difficult to determine the one-way or two-way inclination of TS. Then, this widening of quasi-laminar region will be discussed with energy-spectra in detail.

In order to estimate the effect of the rotation on the structure of TS quantitatively, the streamwise (a, c) and spanwise (b, d) pre-multiplied energy spectra are shown in Fig. 5. Figure 5(a, b) and (c, d) show the results for $\mathrm{Ro}_\tau = 0.0$–0.02, $\mathrm{Re}_\tau = 64$, and $\mathrm{Ro}_\tau = 0.0$, 0.01, $\mathrm{Re}_\tau = 80$, respectively. In this plot, a wavelength of the peak (Most Energetic Wavelength: MEW) represents the size of the most dominant structure. In distributions of k_xE_{uu}, k_xE_{ww} and k_zE_{ww} (a, b), MEW are $\lambda_x^+ = 6500$ and $\lambda_z^+ = 3300$, corresponding to the streamwise (or spanwise) size of TS. In the rotating system ($\mathrm{Ro}_\tau = 0.01$, 0.02), MEW for $\mathrm{Re}_\tau = 64$ of $\lambda_x^+ = 6500$ and $\lambda_z^+ = 3300$ exhibit higher peaks than those in the static system ($\mathrm{Ro}_\tau = 0.0$). This augmentation represents the increase of the energy of TS in the total energy. As for k_zE_{uu} at $\mathrm{Ro}_\tau = 0.0$ in Fig 5(b), in the rotating system, MEW of $\lambda_z^+ = 1600$ at $\mathrm{Ro}_\tau = 0.0$ shifts right and exists at $\lambda_z^+ = 3300$. Then, it proves that the spatial quasi-laminar region, or the acceleration region, becomes wider in the spanwise direction. At $\mathrm{Re}_\tau = 80$, it can be cleary seen that there exists an additional peak at $\lambda_x^+ = 4100$ (or $\lambda_z^+ = 1500$–2000), which corresponds to TS. In point of the difference between the static- and the rotating-systems at $\mathrm{Re}_\tau = 80$, MEW are slightly increased for the weak-rotation case. Especially, MEW in k_zE_{ww} relevant to TS increases clearly due to rotation. Indeed, two MEW corresponding to TS are $\lambda_z^+ = 2000$ and 1500 (which implies the existence of additional MEW between $\lambda_z^+ = 2000$ and 1500) at $\mathrm{Ro}_\tau = 0.0$, but MEW only exists at $\lambda_z^+ = 2000$ for $\mathrm{Ro}_\tau = 0.01$, $\mathrm{Re}_\tau = 80$. With all these factors, in the very-low Ro_τ against the static system ($\mathrm{Ro}_\tau = 0.0$), TS contains more energy in the total energy, whereas the quasi-laminar region is wider. As just described, it is striking that the subjecting very-low rotation number comprehends the paradox that is the augmentation of turbulent energy of TS and the enlargement of quasi-laminar region. The augmentation of turbulent energy would be denoted by quasi-mean spanwise velocity component.

Moreover, Fig. 5 shows the fact that Reynolds-number dependency is more prominant in low-Ro_τ than that in no rotation. The difference in the magnitude of augmentation of TS is responsible to the inclination of TS (one-way or two-way inclination). As shown by flow visualization, the

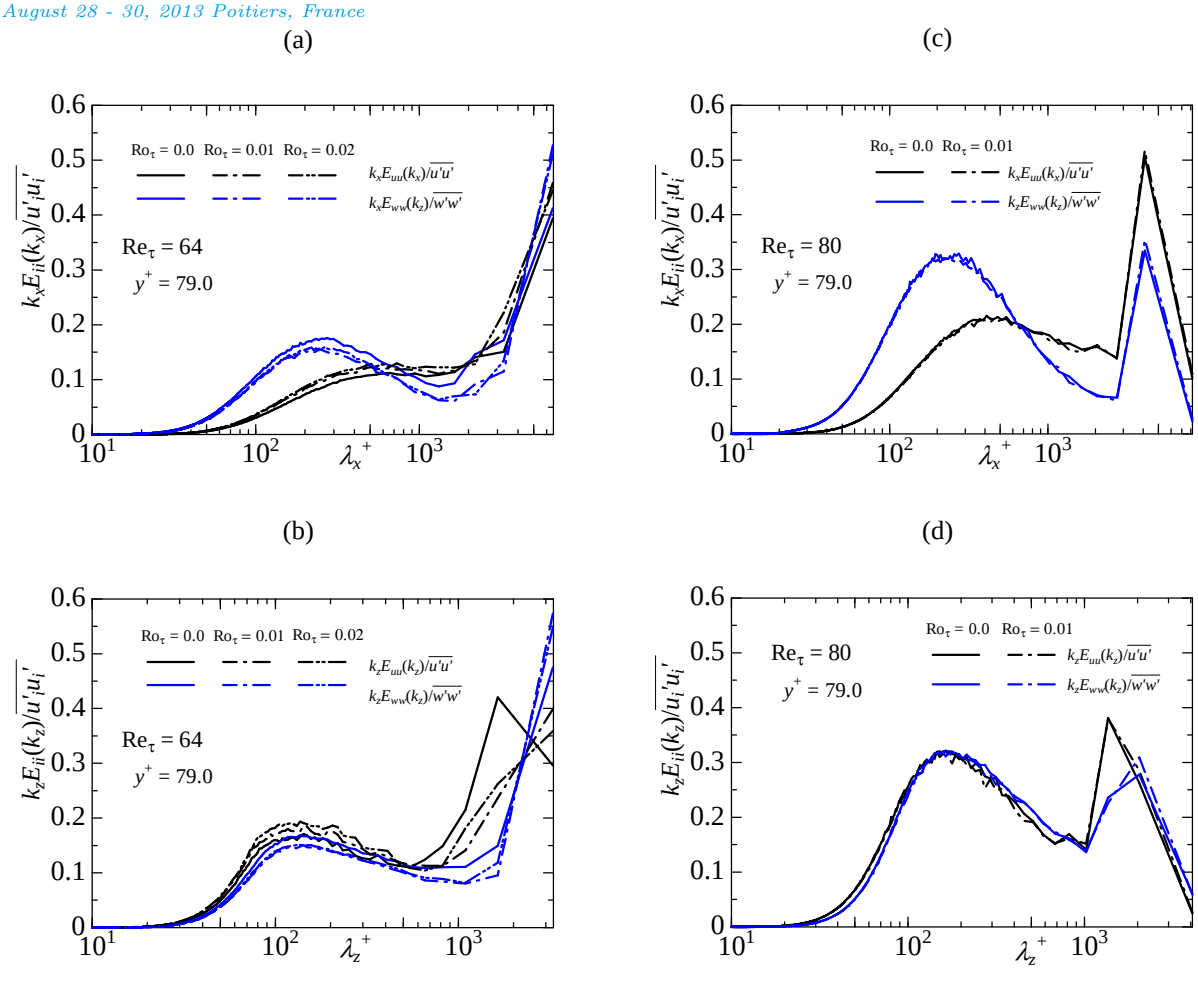

Figure 5. Pre-multiplied energy spectra for u' and w' as a function of either (a, c) streamwise or (b, d) spanwise wavelength (λ_i) at $\mathrm{Re}_\tau = 64$ (a, b) and $\mathrm{Re}_\tau = 80$ (c, d). Note that $k_i = 2\pi/\lambda_i$.

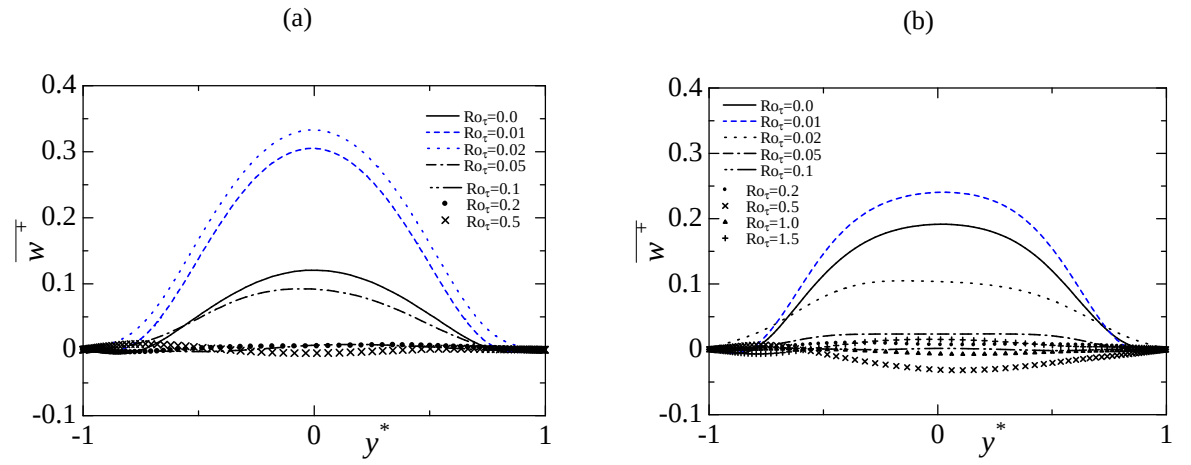

Figure 6. Spanwise mean velocity profiles of $\mathrm{Re}_\tau = 64$ (a) and 80 (b) for various rotation number.

inclinations of TS for $\mathrm{Ro}_\tau = 0.02$, $\mathrm{Re}_\tau = 64$, is one-way inclination while the other cases shown inFig. 4 give two-way inclination. Then, the spatial quasi-laminar region is narrower. At $\mathrm{Ro}_\tau = 0.01, 0.02$, $\mathrm{Re}_\tau = 64$, the inclination results in only one-way inclination. Therefore, the effect of rotation is more remarkable at $\mathrm{Re}_\tau = 64$ than that at $\mathrm{Re}_\tau = 80$. For higher rotation cases, the structure alters from TS to RC, and the peak at the TS wavelength would be attenuated.

Spanwise secondary flow

In this section, let us discuss about statistics relating to the spanwise velocity component which characterizes TS. Figure 6 shows the spanwise mean velocity profile ($\overline{w^+}$). It is known that this averaged value should become zero in the turbulent or the laminar channel flow. As the existing results, $\overline{w^+}$ becomes about zero in high-Ro_τ, because of the dominant of RC. However, ($\overline{w^+}$) has significant magnitude

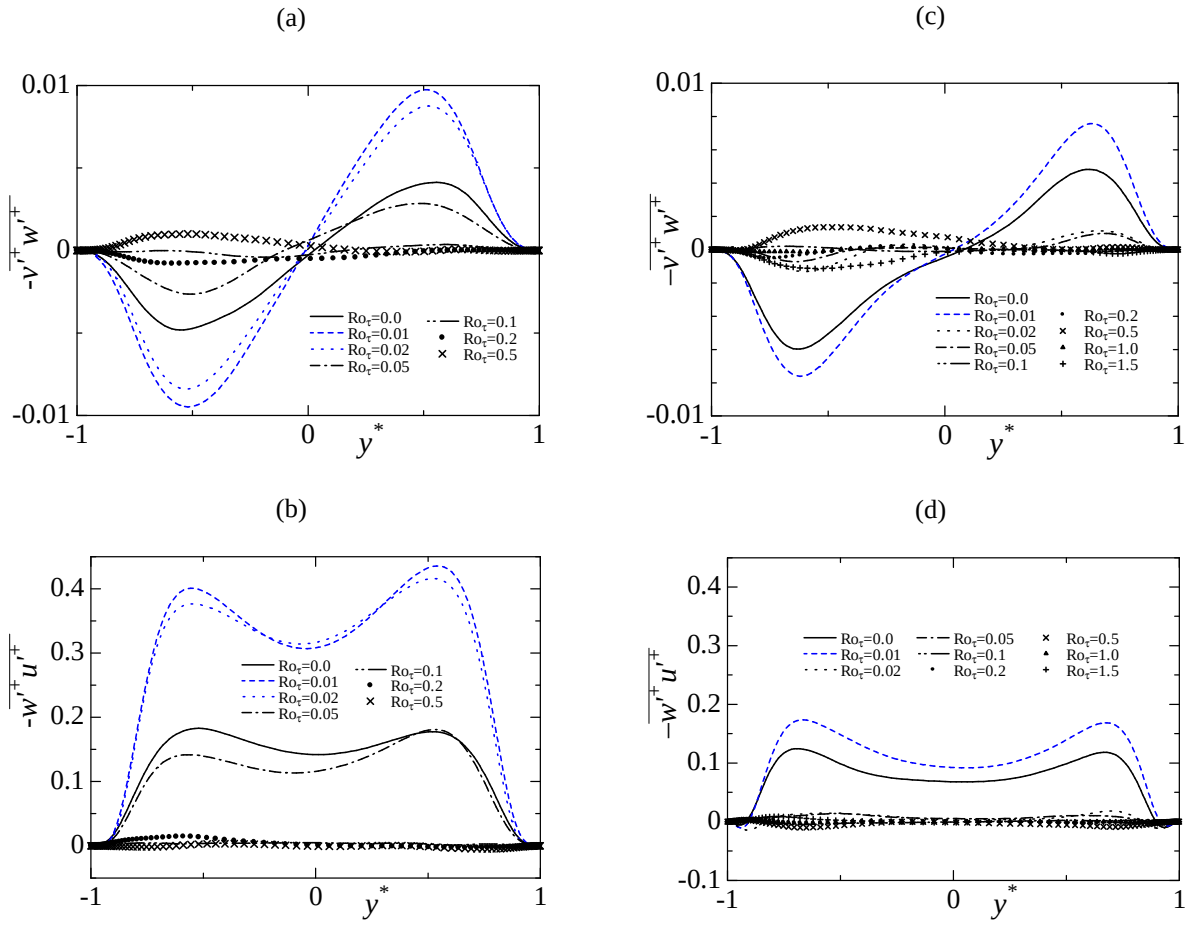

Figure 7. Wall-normal profiles of Reynolds shear stress at $\mathrm{Re}_\tau = 64$ (a, b) and 80 (c, d): $-\overline{v'^+w'^+}$ (a, c), $-\overline{w'^+u'^+}$ (b, d).

in the flow state accompanied by TS in both of the pressure and suction sides because spanwise secondary flow occurs along each turbulent band of TS. The spanwise secondary flow is induced by the impingement of quasi-laminar and turbulent region (this mechanism is shown in Fig 3). The impingement causes flow redirection from the streamwise to the spanwise direction, and TS has strong velocity component. Hence TS disappears when the spanwise velocity component is broken off. It is known that, TS occurs only in high-aspect ratio about x and z directions for y direction, and TS does not occur in the case of low-aspect ratio such as duct flow, since $\overline{w^+}$ is dampened.

As see in Fig 6, $\mathrm{Ro}_\tau = 0.0$ reveals non-zero value of $\overline{w^+}$ through the channel because of the occurrence of TS. It is interesting to note that, at $\mathrm{Ro}_\tau = 0.01$, 0.02, $\mathrm{Re}_\tau = 64$ and $\mathrm{Ro}_\tau = 0.01$, $\mathrm{Re}_\tau = 80$ (blue lines) they are significantly increased compared with those at $\mathrm{Ro}_\tau = 0.0$. Considering the Re_τ dependency, at $\mathrm{Re}_\tau = 64$ where TS is dominant, the value of $\overline{w^+}$ change due to rotation is larger than those at $\mathrm{Re}_\tau = 80$, and the w^+ value is highest. Under the spanwise system rotation, the Coriolis instability would not directly affect the spanwise velocity component as mentioned above (see in Introduction). In this cases (only in very-low Ro_τ at which TS occurs), $\overline{w^+}$ increases with rotation. Thus, the direct effect does not have so much of an impact on the velocity component in very-low Ro_τ. This alteration is attributable to the indirect Coriolis effects, which involves the suppression of an energy cascade from a low to a high wavenumber. The indirect effect enhances TS because TS contains long-wavelength as discussed in Fig 5. At only a low Ro_τ, the indirect effect should be stronger than the direct effect, and thus the spanwise velocity component might increase. Indeed, we confirmed that turbulent energy is maintained and augmentation in the long-wavelength region responding to TS as a result of very-low rotation effect. In addition, that long-wavelength is longer. Consequently, the spatial region where the flow variance arises to the spanwise component is wider, because the spatial quasi-laminar region is enlargement.

The Reynolds shear stresses of $-\overline{v'^+w'^+}$ and $-\overline{w'^+u'^+}$ at $\mathrm{Re}_\tau = 64$ and 80 for different Ro_τ are given in Fig. 7. As can be seen in Fig. 6, the values of $-\overline{v'^+w'^+}$ and $-\overline{w'^+u'^+}$ are about zero in the turbulent or the laminar-channel flow. Otherwise, in the occurence of TS, they are non-zero values. At only in very low $\mathrm{Ro}_\tau (= 0.01, 0.02$ at $\mathrm{Re}_\tau = 64$ and 0.01 at $\mathrm{Re}_\tau = 64)$, those values are higher than $\mathrm{Ro}_\tau = 0.0$. In detail, the peak values of $-\overline{v'^+w'^+}$ and $-\overline{w'^+u'^+}$ are higher at $\mathrm{Re}_\tau = 64$ than those at $\mathrm{Re}_\tau = 80$ irrespective of the static or rotating system. Under the spanwise system rotation, the Coriolis instability would not affect directly the spanwise velocity component as mentioned above, but would give rise to the longitudinal vortices (of RC) in the unstable (pressure) side. The enhancement of the shear stresses including w' in the whole channel (irrespective of the stable and the unstable side) implies the augmentation of the TS structure, which is practically uniform in the wall-normal direction from the viewpoint flow state.

At last, we discuss about the high rotation number

ranges. When Ro_τ increases, the peak value of the spanwise velocity component decreases (see in Figs. 6 and 7). This reduction is caused by the development of RC. The structure of RC is large-scale longitudinal vortices and causes variation of the wall-normal velocity component. On the contrary, TS does not contain intensive wall-normal velocity component. The wall-normal turbulent intensity increases against the spanwise component by the development of RC, and then TS disappears.

CONCLUSION

We discussed the effects of spanwise rotation on the structure of turbulent stripe in PPF ($\mathrm{Ro}_\tau = 0.0$) and in RPPF ($\mathrm{Ro}_\tau > 0.0$) for transitional Reynolds numbers ($\mathrm{Re}_\tau = 64$ and 80), and drew the following conclusions.

— The structure of TS occurs only in flows with weak or no spanwise system rotation. In the case of Ro_τ as low as 0.01 and 0.02 at $\mathrm{Re}_\tau = 64$ and as 0.01 at $\mathrm{Re}_\tau = 80$, the Coriolis instability enhanced the structure of TS.
— The states of TS are clasiffied into two patterns: they are one-way and two-way inclinations of TS, which is relevant to the spatial size of the quasi-laminar region. The quasi-laminar region in the case of the one-way inclination is wider than that for the two-way inclination.
— In the very-low Ro_τ,the wavelength corresponding to TS size has more energy than in the static system, whereas the quasi-laminar region is wider.
— The augmentation phenomenon of TS is caused by the Coriolis indirect effect. The structure of TS is equivalent to MEW at the wavelength much longer than turbulent fine-scale eddies. The energy of TS is maintained and augmented in the long wavelength region by indirect effect.
— The spanwise secondary flow occurs along each turbulent band of TS. In addition to the spanwise component such as $\overline{w^+}$, $-\overline{v'^+ w'^+}$ and $-\overline{w'^+ u'^+}$ are increased by low-rotation with the ocurence of TS in both of the pressure and suction sides. When Ro_τ is further increased to the level of the RC occurrence, $\overline{w^+}$ and the shear stresses including w' decrease, resulting in disappearence of TS.

The occurrence of TS is important from the viewpoint of mass and heat transport in the spanwise direction because the spanwise velocity component has a distinguished value. It would be impossible in the featureless turbulence or the laminar flow, since the mean spanwise velocity component is zero. The present study demonstrates that the system rotation even with very low Ro_τ gives rise to non-zero mean spanwise velocit. It is favorable to the engineering application because of efficient transfer by TS.

This work was supported by a KAKENHI Grant-in-Aid, #22760136 and TEPCO (Tokyo Electric Power Company) Memorial Foundation. The present simulations were performed by SX-9 at Cyberscience Center, Tohoku University.

REFERENCES

Bradshaw, P., 1969, “The analogy between streamline curvature and buoyancy in turbulent shear flow”, J. Fluid Mech., Vol. 36, pp 177-191.

Brethouwer, G., Duguet, Y., and Schlatter, P., 2012 “Turbulent-laminar coexistence in wall flows with Coriolis, buoyancy or Lorentz forces”, J. Fluid Mech., Vol. 704, pp 137-172.

Hashimoto, S., Hasobe, A., Tsukahara, T., Kawaguchi, Y., and Kawamura, H., 2010, “An experimental study on turbulent-stripe structure in transitional channel flow”, Proceedings of 6th International Symposium on Turbulence, Heat and Mass Transfer, pp. 193-196.

Ishida, T., Tsukahara, T., and Kawaguchi, Y., 2013, “DNS of rotating turbulent plane Poiseuille flow in low Reynolds- and rotation-number ranges”, Proceedings of iTi2012, Progress in Turbulence., in press.

Johnston, J.P., Halleen, R.M., and Lezius, D. K., 1972, “Effects of spanwise rotation on the structure of two-dimensional fully developed turbulent channel flow”, J. Fluid Mech., Vol. 56, pp. 533–557.

Lezius, D. K. and Johnston, J.P., 1976, “Roll-cell instabilities in rotating laminar and turbulent channel flow”, J. Fluid Mech., Vol. 77, pp. 159–175.

Morinishi, Y., Nakabayashi, K., and Ren S. Q., 2001, “Dynamics of anisotropy on decaying homogeneous turbulence subjected to system rotation”, Phys. Fluids, Vol. 13, No. 10, 2912.

Tsukahara, T., Kawaguchi, Y., Kawamura, H., Tillmark, N., and Alfredsson, P. H., 2010, “Turbulent stripe in transitional channel flow with/without system rotation”, Proceedings of 7th IUTAM Symposium, Laminar-Turbulent Transition, IUTAM Book series, Vol. 18, pp. 421-426.